Chapter 15

Surface-Barrier Photodiodes with Transparent Electrodes for High-Performance Detection in the UV-NIR Spectrum

Oleksandr Malik and
Francisco Javier De la Hidalga-Wade

Additional information is available at the end of the chapter

http://dx.doi.org/10.5772/67469

Abstract

The aim of this chapter is to present a short review in the field of design, fabrication technology, and testing of high-efficiency surface-barrier photodiodes with electrodes based on thin-film transparent conducting oxides (TCO) such as tin-doped indium oxide (ITO) and fluorine-doped tin oxide (FTO). Most of this review is based on our own results obtained and reported during the last 30 years. Besides a brief description of the low-cost spray pyrolysis deposition technique, mainly used in our work for deposition of the TCO films on a semiconductor surface, structural, morphological, and optoelectronic properties of these TCO films are discussed. As an example, a successful application of these TCO films is shown and used in high-efficiency surface-barrier photodiodes for a wide spectral range, from near ultraviolet (UV) to near infrared (NIR), and fabricated on different semiconductor substrates such as traditional Si, wide energy band ZnS, and GaP compound semiconductor substrates. The possible use of the Si surface-barrier structures as radiation-resistant detectors and gamma radiation detectors is discussed. The properties of high-efficiency surface-barrier photodiodes based on a perspective ternary semiconductor compound, $Hg_3In_2Te_6$ mercury indium telluride (MIT), for detection of 1.3 μm and 1.55 μm radiation for applications in fiber optics, are also reported.

Keywords: surface-barrier photodetectors, thin film, tin-doped indium oxide, fluorine-doped tin oxide, spray pyrolysis

1. Introduction

Physics of surface-barrier (SB) devices is based on the well-known Schottky barrier, named after Walter H. Schottky, which is a potential energy barrier for carriers formed at a metal-semiconductor

(M-S) junction [1]. In the design of SB photodetectors, the main function of the barrier is to separate carriers photogenerated inside the semiconductor substrate. Such photodiodes are very simple device structures; because a p-n junction is not necessary, it does not present optical losses in the highly doped p-layer and also present a very high speed of response on modulated optical signal. The SB structure is very useful for fabrication of optoelectronic devices on semiconductors, in which a p-n junction cannot be created due to doping troubles. At the same time, in order to use M-S structures as radiation detectors, the metal electrode needs to be extremely thin (<15 nm) to avoid the radiation absorption losses and also must be chemically resistant to prevent device degradation in time. A thinner metallization leads to devices susceptible to degradation. Among all the metals, only some of them such as Au, Pt, and Ni are suitable for this application. Moreover, the high reflectivity of these metallic layers demands the use of antireflection coatings. The electrical properties of SB photodetectors based on M-S structures in many cases can be enhanced by the introduction of a very thin (<3 nm) insulating layer between the metallic film and the semiconductor (M-I-S structures). The presence of this insulator layer reduces the number of localized states at the semiconductor interface and hence serves to reduce interface carrier recombination. Its presence can also reduce significantly thermionic emission current because of an increase in the potential barrier for majority carriers [2]. At that, the thickness of the insulating layer must not reduce the transport of minority carriers from the semiconductor to the metal.

For best photoelectrical properties of SB radiation detectors based on M-S and M-I-S structures, the metallic opaque layer can be changed by a thin film based on some transparent conducting oxide (TCO), such as tin-doped indium oxide (ITO) or fluorine-doped tin oxide (FTO), which are widely used for optoelectronic applications. Such films can be deposited on a semiconductor surface by different technological methods as thermal vacuum deposition, e-beam deposition, sputtering, chemical vapor deposition, sol-gel deposition, and spray pyrolysis [3]. Spray pyrolysis is a low-cost and simple technological method used successfully since 1976 for the fabrication of efficient solar cells based on metal oxide (ITO, FTO)-silicon structures [4–11]. In such structures, the TCO films work as an active metal-like transparent conducting electrode. Thickness tuning of the TCO films allows for its use as an effective antireflection coating for reducing radiation losses.

In this chapter we pay attention to application of spray-deposited ITO and FTO films for fabrication of high-efficiency SB photodetectors for applications in a wide spectral region. The material presented in this chapter is based on original results reported in this field during the last 35 years; hence, this review will be very useful for a large number of readers.

2. Spray pyrolysis processing

Spray pyrolysis [12] is a process in which a thin film is deposited by spraying a solution on a heated surface, where the constituents react to form a chemical compound. The chemical reactants are selected such that the products other than the desired compound are volatile at the temperature of deposition. Usually, two types of processing are used: the process in which the droplet resides on the surface as the solvent evaporates, leaving behind a solid that may further react in the dry state and the process where the solvent evaporates before the droplet reaches the surface and the dry solid impinges on the surface, where decomposition occurs.

http://dx.doi.org/10.5772/67469

Three sprayed solution were used for photodetectors fabrication. The ITO films were deposited from solution contents 13.5 mg of $InCl_3 \times 4H_2O$ dissolved in 170 ml of water and ethylic alcohol (1:1) mixture, with an addition of 5 ml of HCl to prevent hydrolysis. The different ratios of Sn/In in the solution were controlled by adding in the solution a calculated amount of tin chloride ($SnCl_4 \times 5H_2O$) [13]. As alternative, the ITO layers can be deposited by spraying a solution of Indium (III) acetate, $In(OOCCH_3)_3$ dissolved in ethanol at 25°C by adding Tin(IV) chloride, $SnCl_4 \times 5H_2O$, and HCl. Ratio Sn/In in the solution varied by calculated amount of tin chloride. A glass atomizer was designed in order to produce small-size droplets. The spraying was conducted using compressed air. Substrates were placed on heater having fixed temperature of 460 ± 2°C. The heater was covered with polished carbon disk having a high thermal conductivity and chemical resistance in order to assure a uniform temperature of the substrates. The substrate temperature was controlled with a thermocouple. The optimum distance from the atomizer to the substrate and the compressed air pressure were 25 cm and 1.4 kg/cm^2, respectively. In order to prevent the deposition of the films under nonequilibrium thermal conditions, due to a possible fast cooling of the substrate surface with the stream of the precursor and the compressed gas, periodical cycles of the deposition, with durations of 1 sec and intervals of 10 sec, were employed.

Fluorine-doped tin oxide (FTO) films [14] were deposited from solution contents a 0.2 M solution of tin chloride ($SnCl_4 \times 5H_2O$) dissolved in methanol. A small amount of NH_4F dissolved in water was added in the starting solution for the preparation of the precursor with 0–1 F/Sn molar concentrations. A few drops of HCl were added to the precursor solution in order to prevent the hydrolysis of the tin chloride due to the presence of water. The flow rate of the precursor during the deposition process was 10 ml/min. Other deposition parameters were the same as for the ITO films.

For fabrication of the M-S or M-I-S structures, the ITO and FTO films were deposited on chemically prepared surface of semiconductor substrates. A Corning glass or sapphire substrates placed on the heater together with the semiconductor substrates were used as referents for the measurement of the films' properties. The structural characterization of the ITO films was conducted using a Bruker D8 Advanced X-ray diffractometer (XRD), with Cu K_α radiation (λ = 0.15406 nm). The morphological features of the ITO films were examined using the Ambios USPM atomic force microscope (AFM). Keithley's Series 2400 Source Measurement Unit and the Ecopia HMS-5000 Hall Effect Measurement System were used for electrical characterization. The optical measurements were carried out using the F20 Filmetrics and the Agilent 8453 spectrometers.

3. Properties of the metal oxide films

Both, the ITO and FTO films deposited with conditions described above were microcrystalline. X-ray diffraction (XRD) spectra for films with optimal doping concentration are shown in **Figure 1**.

The optimal doping concentration for the ITO and FTO films means the value of doping at which is obtained the lowest sheet resistance $R_s = \rho/d$, where ρ and d are the film resistivity and thickness,

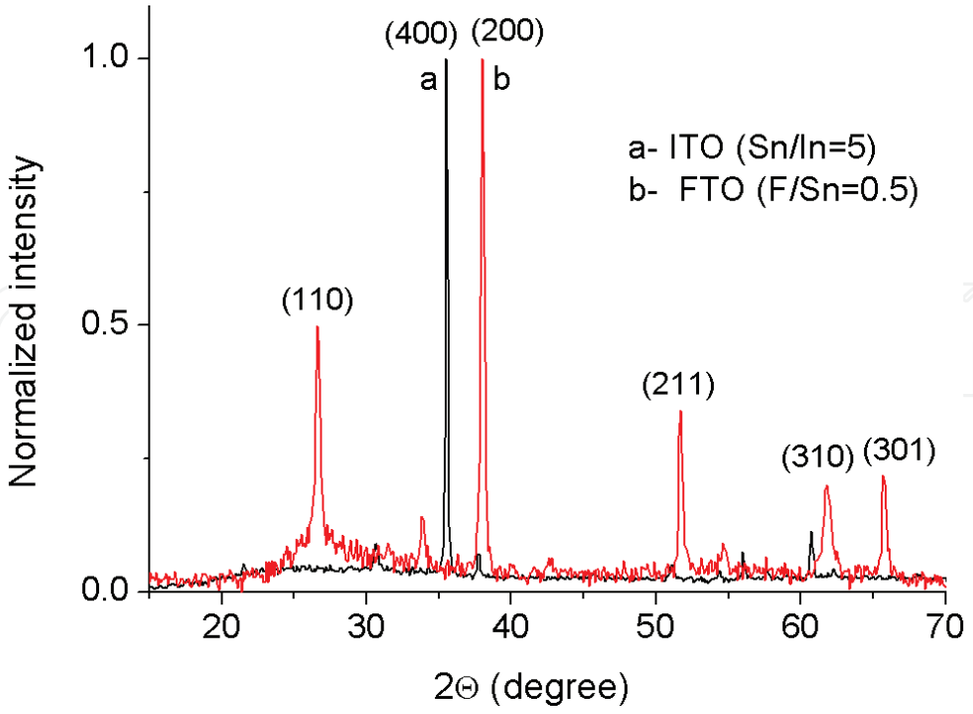

Figure 1. XRD patterns for sprayed ITO and FTO films.

respectively. At the same time, the value of transmittance (T) is important. For practical applications of the TCO films as transparent conducting electrodes, the fabrication process needs to be optimized for obtaining a better balance between R_s and T. However, a simultaneous obtaining of maximum transmission and conductivity is not possible to achieve in most cases. Haacke [15] proposed the figure of merit (FOM) $\phi_{TC} = T^{10}/R_s$ for comparison of films with different thickness and fabrication histories. A higher FOM value indicates a higher performance; this characterizes a film showing simultaneously a low sheet resistance (R_s) and a high transparency (T). However, the value of one of these parameters can compromise the value of the other. To avoid influence of an interference effect in the thin films, the average integrated value of the films transmittance (T_{int}) at wavelengths in the 400–700 nm spectral range is better to be used for the FOM value calculation. **Table 1** presents structural, electrical, and optical parameters of the ITO and FTO films deposited at 460°C from the solutions containing the optimal doping concentration.

The parameters obtained allow to conclude that high-quality FTO and ITO films can be fabricated by a simple and inexpensive spray deposition method. Our recently published works [13, 14] give more detailed information about the dependence of the film properties on the doping concentration as well as a comparison of our results with the ones published in literature.

FTO and ITO are degenerated wide band gap semiconductors. Films of these materials can be used as transparent conducting electrodes in ultraviolet (UV) SB photodetectors. In nominally doped semiconductors, the Fermi level lies between the conduction and valence bands. As the doping concentration is increased, electrons populate states within the conduction band which pushes the Fermi level higher in energy, and in the case of degenerate level of doping, the Fermi level lies inside the conduction band. At that, using transmission/reflection spectroscopy, the

Parameters	Spray deposited FTO film	Spray deposited ITO film
Ratio F/Sn in solution	0.5	–
Ratio Sn/In in solution	–	5
Preferred grain orientation	200	400
Grain size (nm)	120	110
Specific resistance (10^{-4} Ω cm)	1.8	2
Carrier concentration (10^{20} cm^{-3})	16.0	11.5
Mobility ($cm^2V^{-1}s^{-1}$)	21.0	28
Integrated transmittance (T_{int})	0.84	0.85
FOM (10^{-3} Ω^{-1})	38	20

Table 1. Comparison properties of the FTO and ITO films deposited by spray pyrolysis from the solutions with optimal doping concentration (ratio of F/Sn and Sn/In).

optical energy gap (E_{opt}) can be measured. This value is not coinciding with value E_g that is a distance between the valence and conduction bands as is shown in **Figure 2**. The difference ΔE is named as Burstein-Moss shift [16]. In the case of a degenerate semiconductor, an electron from the top of the valence band can only be excited into conduction band above the Fermi level (which now lies in conduction band) since all the states below the Fermi level are occupied states. Pauli's exclusion principle forbids excitation into these occupied states. The value of ΔE is proportional to the carrier concentration. Burstein-Moss shift for FTO and ITO films, characteristics of which are shown in **Table 1**, is 0.5–0.8 eV. At that, the value of optical energy gap determined from analysis of transmittance (**Figure 3**) for the FTO and ITO films is 4.3 eV and 4.8 eV, respectively. From **Figure 3** we made an important conclusion that FTO films are more suitable for UV SB photodetectors.

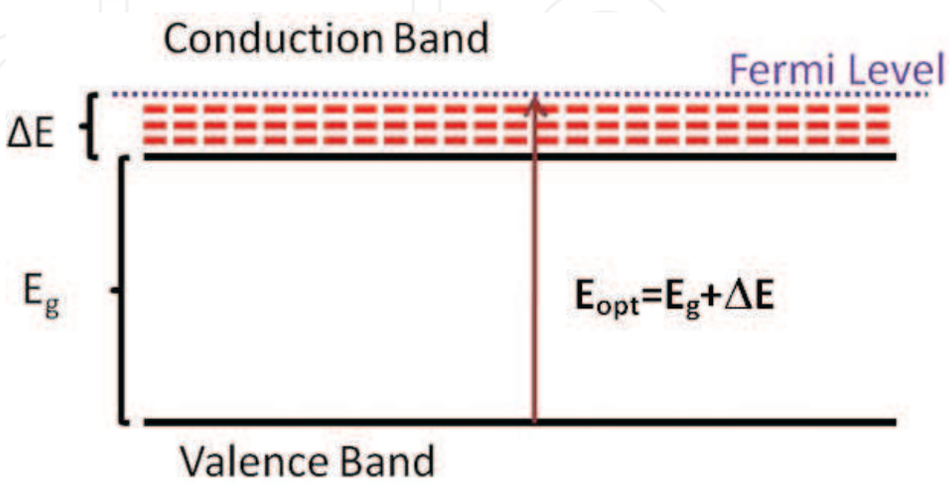

Figure 2. Illustration of the Burstein-Moss shift in degenerated semiconductors.

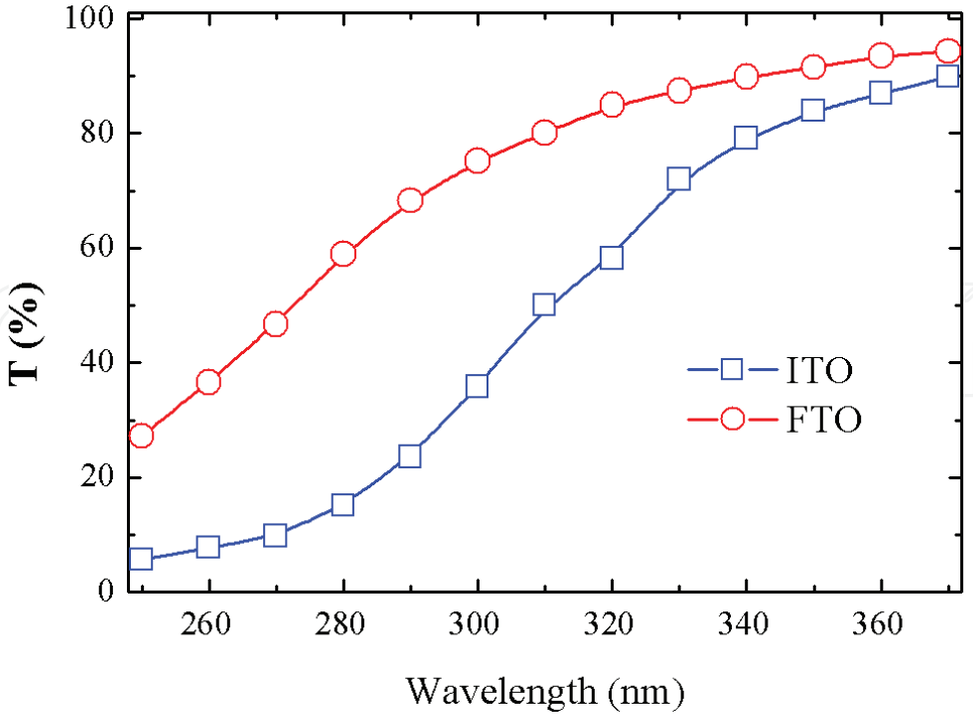

Figure 3. Transmittance of FTO and ITO films in the UV spectral range.

4. Surface-barrier photodetectors for the UV spectral range

There are many applications (biomedical, astronomy, flame safeguard systems, and others) that require the measurement of blue or UV radiation in the presence of visible light. The spectral selectivity of photodiodes depends on a band gap of semiconductor which is shown in **Figure 4**.

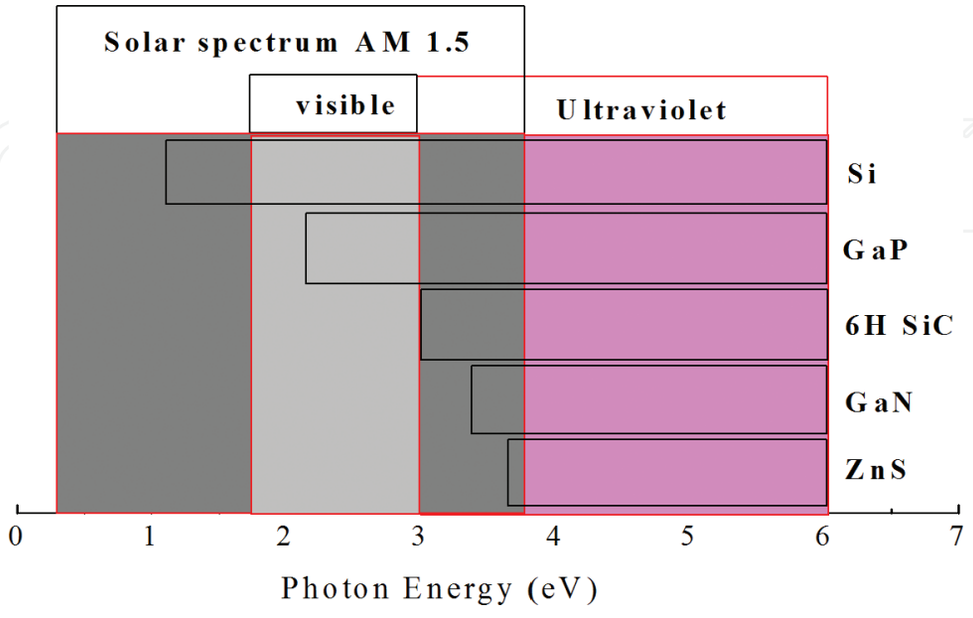

Figure 4. Semiconductors of interest for visible, UV, and solar-blind photodetectors.

http://dx.doi.org/10.5772/67469

In this direction, researchers are paying attention to large-band-gap semiconductor compounds such as GaP, SiC, and GaN in contrast to Si-based photodiodes in which the selectivity can be provided with additional blocking filters or dielectric coating to fit them with the spectral region of interest.

4.1. Solar-blind UV photodetectors based on monocrystalline ZnS

The large-band-gap (3.6 eV) zinc sulfide (ZnS) greatly reduces the sensitivity to photons in the terrestrial solar radiation, and it is an attractive material for developing solar-blind photodetectors.

N-type ZnS monocrystalline wafers were used for the fabrication of ITO-ZnS and FTO-ZnS [17, 18] UV SB photodetectors, with active areas ranging from 5 to 100 mm^2. FTO and ITO films have been deposited at the top surface of the monocrystals by spray technique at conditions described in Section 2. The backside ohmic contact to the ZnS was made as described in [17]. The current-voltage characteristic of FTO-ZnS photodetector with an area of 1 cm^2 is shown in **Figure 5**.

Figure 6 shows the spectral response of the FTO-ZnS photodetector [18] in comparison with characteristic of ITO/ZnS [17] and SiC [19] UV photodetectors.

In contrast to ITO-ZnS detectors, the maximum spectral sensitivity peak of the FTO/ZnS photodetectors shifted from 330 to 290 nm, due to the higher transparency of the FTO layer in UV, when compared to the transparency of the ITO layer (**Figure 3**). The combination of a low dark current and a high sensitivity originates a low value for the noise-equivalent power (NEP), ranging from 10^{-14} to 10^{-12} W/Hz$^{1/2}$, that is a function of the area of the sensors. In **Figure 7**, the

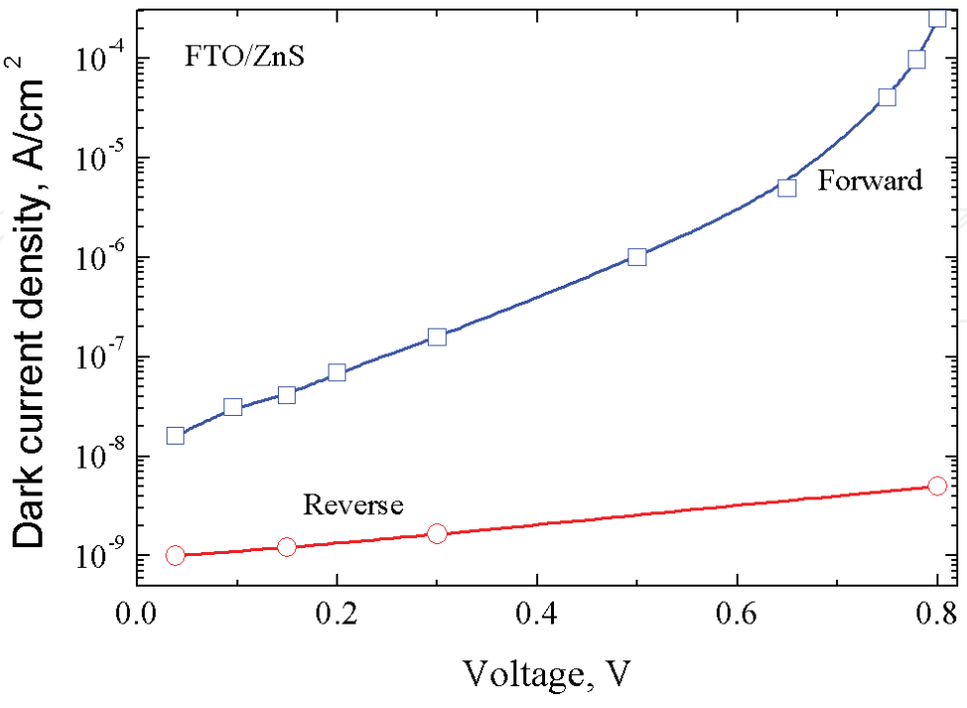

Figure 5. Current-voltage characteristic of FTO-ZnS photodetector with an area of 1 cm^2.

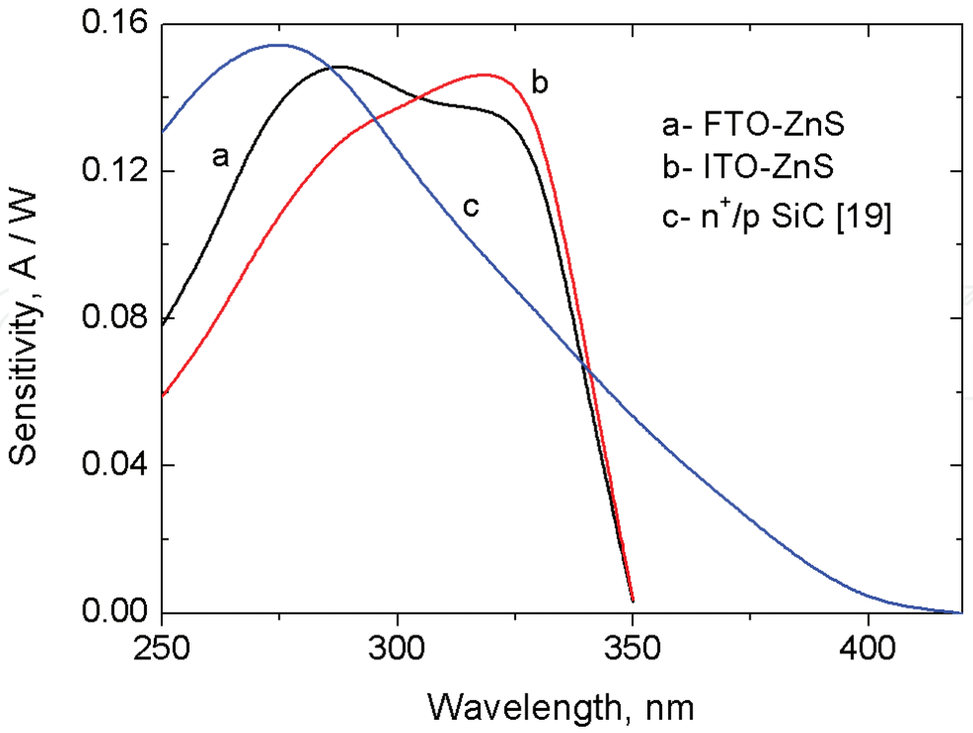

Figure 6. Spectral sensitivity of FTO-ZnS and ITO-ZnS photodetectors in comparison with a SiC UV photodetector [19].

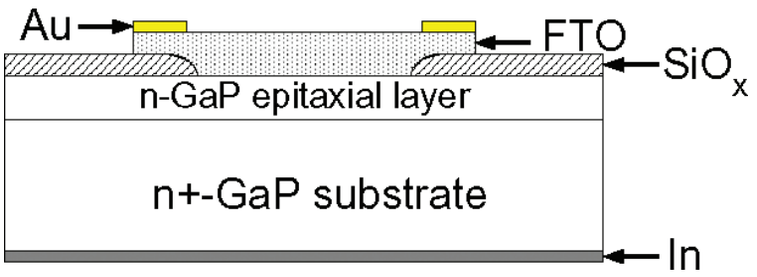

Figure 7. Schematic cross section of the FTO/n-n$^+$ GaP SB photodetector.

dependence of the photocurrent on incident light power is shown. A linear dependence of photocurrent on incident light power ranging from 10^{-8} to 10^{-3} W was found.

Thus, SB UV FTO-ZnS photodetectors show excellent characteristics as solar-blind UV detectors with high, 66%, external quantum efficiency, and can be used for different technical applications without losing their photoelectrical parameters under direct solar irradiation.

4.2. UV photodetectors based on epitaxial GaP

Our research results about SB photodetectors with transparent TCO electrode deposited by spray pyrolysis technique on gallium phosphide (GaP) with a band gap 2.27 eV were reported during the last 20 years [20–24]. Here, a brief resume of these works in comparison with reported by other authors is done.

http://dx.doi.org/10.5772/67469

A simple and low-cost pyrolysis technique has been used to form the high transparent conducting FTO or ITO electrode on prepared surface of GaP n-n^+ epitaxial structures with 10–12 μm thick epitaxial layers. The estimated electron density in the epitaxial layer is around 10^{16} cm^{-3}. The back ohmic contact was formed by indium diffusion. **Figure 7** shows the schematic cross section of a photodiode based on the FTO-GaP heterostructure.

The typical dark current-voltage (I-V) characteristic of the FTO-GaP photodiode with an active area of 3 mm^2 measured at room temperature is shown in **Figure 8**.

The results show excellent junction properties of FTO-GaP photodiodes. The equivalent shunt resistance R_{sh}≈100 GΩ was evaluated at a bias ±50 mV, and this resistance is a main source of the

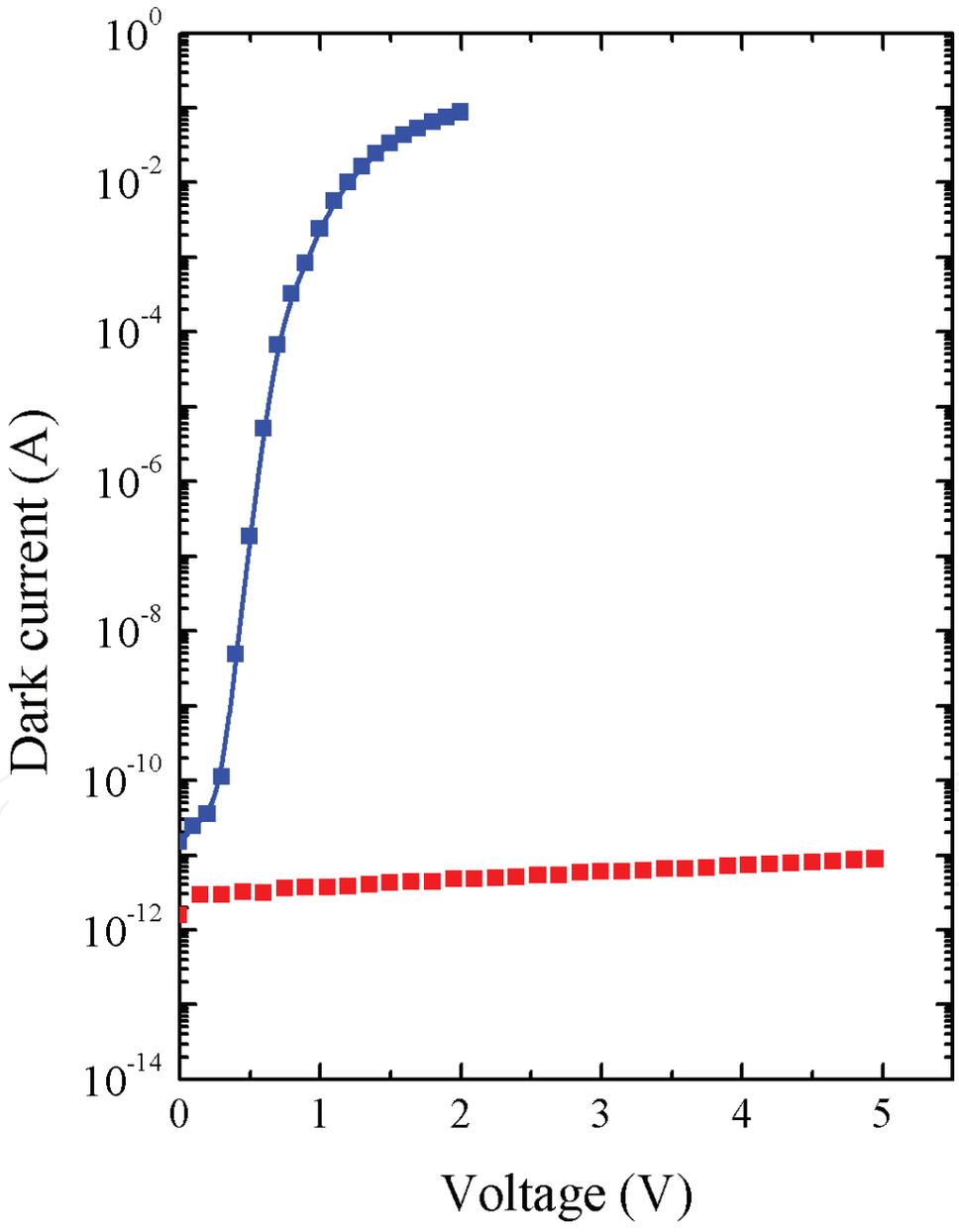

Figure 8. The typical I-V characteristics of FTO-GaP photodetector.

device noise, which limits the detectivity in short-circuit current mode. The FTO film resistance causes the non-exponential current increasing at forward bias higher than 0.6 V. A saturation current of $I_o \approx 10^{-15}$ A and an ideality factor $n = 1.1$ were determined from the exponential region of the forward I-V characteristic. The donor concentration $N_D = 3.8 \cdot 10^{16}$ cm^{-3} and the built-in potential $V_{bi} = 1.33$ V in the GaP epitaxial layer were determined from the C-V characteristics at 10^3 Hz. The thickness of FTO film is an important factor for spectral sensitivity of the developed photodetectors due to the possibility using this film as an effective antireflection coating. The spectral sensitivity of FTO-GaP SB photodetectors having different thicknesses of the FTO electrode as well as ITO-GaP photodetector with 65 nm thick ITO film is shown in **Figure 9**.

The typical performance parameters of the photodiodes with TCO layer are summarized in **Table 2**. The maximal spectral sensitivity depends on the thickness of the TCO film.

Maximal sensitivity of commercial GaP photodetectors based on Au-GaP Schottky barriers (G1962, EDP-365-0-2.5, JEP 5-365) fabricated by well-known companies Hamamatsu, Roithner LaserTechnik, and electro optical components (EOC) lies in the range of 0.07–0.12 A/W with electric parameters that do not exceed as reported here. More close parameters were rep orted for Ag-GaP photodetectors [25]; maximal spectral sensitivity of which was reported as 0.12 A/W.

High-efficient FTO-GaP photodetectors [23] have been used in the design of the radiometric heads of the UVR-21 UV radiant power meter [26]. The UVR-21 UV (**Figure 10**) is an easy-to-use, handheld power meter with unique future intended to make the calibrated measurements of UV-A, UV-B, and UV-C radiation. At the heart of the URV-21 is spectral-filtered

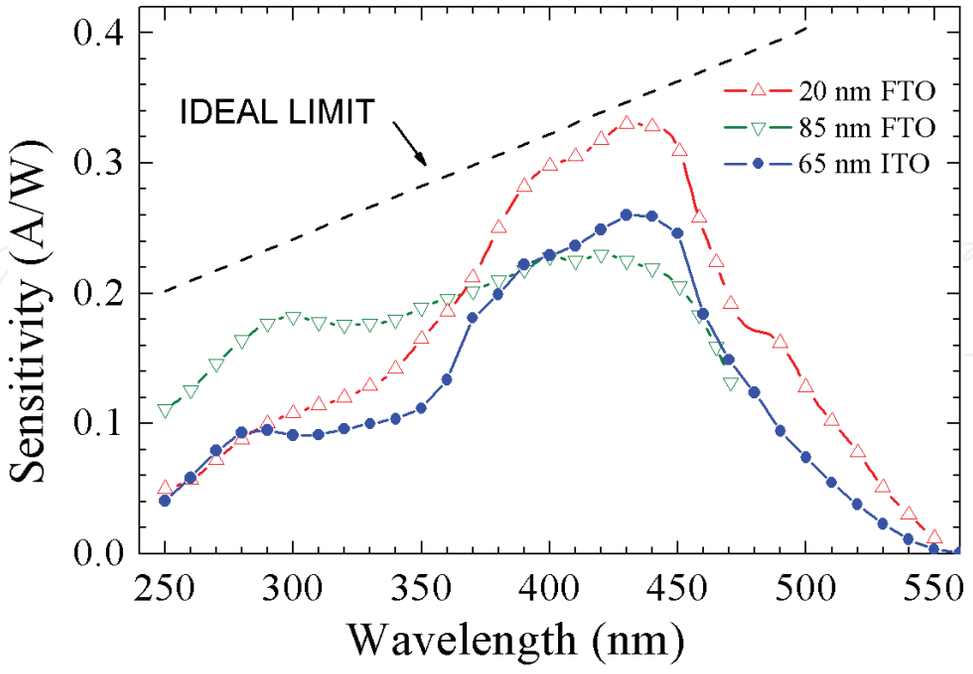

Figure 9. The spectral sensitivity of FTO-GaP and ITO-GaP SB photodetectors for different thicknesses of the transparent conducting electrode.

http://dx.doi.org/10.5772/67469

Electrode material	FTO	ITO
Active area (mm^2)	3	3
Terminal capacitance (nF)	2	1.5
Dark current at V = 1V (pA)	2	20
Shunt resistance (GΩ)	100	30
Peak sensitivity wavelength (nm)	439	435
Peak sensitivity (A/W)	0.2–0.26	0.2–0.26
Peak quantum efficiency (%)	57–74	57–74
Noise-equivalent power ($W/Hz^{1/2}$)	1.7×10^{-15}	3×10^{-15}

Table 2. Comparison of the properties of photodetectors with FTO and ITO electrodes deposited by spray pyrolysis.

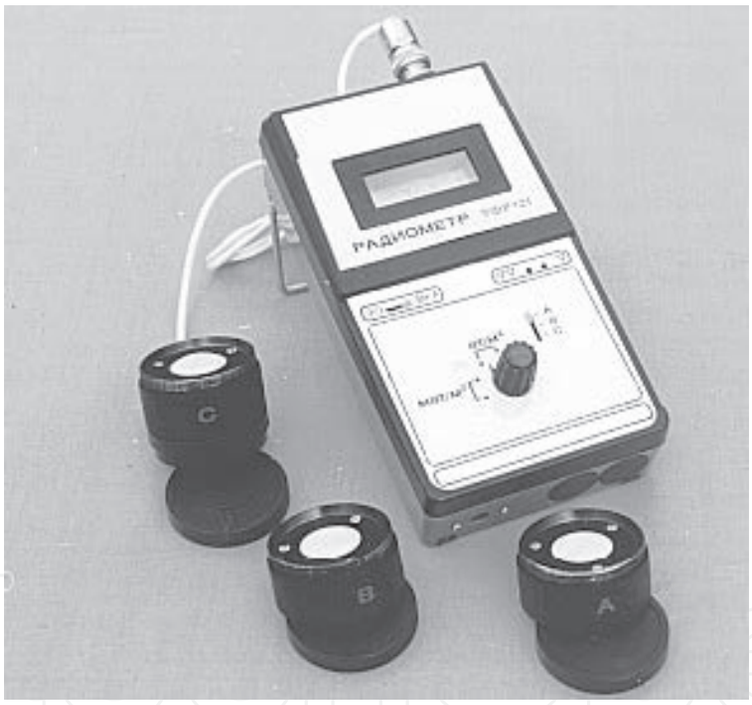

Figure 10. A handheld UV radiant power meter UVR-21 with FTO-GaP–based radiometric heads.

FTO-GaP-based radiometric heads. The interference filters to select requirement spectral band were fabricated on quartz substrates by vacuum deposition. The interchangeable UV radiometric heads allow measuring UV-A, UV-B, and UV-C radiation in the range from 10^{-3} to 10^{3} Wm^{-2}. A rechargeable NiCd battery life is 6–8 hours. Specification limit of measurement relative error is less than 5%.

The performance data of UV radiometric heads are shown below.

Spectral range (nm)		
UV-C radiometric head	220	280
UV-B radiometric head	280	315
UV-A radiometric head	135	400
Irradiance range (Wm^{-2})	10^{-3}	10^{3}
Linearity error (%)		<1
Response uniformity (%)		<1
Measurement error (%)		<5
Cosine error (%) at zenith angle		
30°		3
60°		7
80°		15

5. Silicon surface-barrier photodetectors for visible and near-infrared spectral range

The first results about silicon photodiodes were published more than 60 years ago, and the first detailed investigations of the silicon surface-barrier diodes with thin gold electrode have been published in 1962 [27, 28] by researches from the USA. The first superior electric and photoelectric characteristics of SnO_2-Si heterojunction diodes fabricated by a simple process of spraying a solution containing a tin compound were published in 1975 [29] by authors from Japan.

In this chapter, a brief review of our original results [30, 31] in the field of different types of SB silicon photodetectors with transparent conducting FTO and ITO electrodes is shown.

5.1. Fabrication, properties, and applications of FTO-Si surface-barrier photodetectors

The main technological fabrication steps of FTO-Si photodetectors are shown in **Figure 11**.

Photodetectors were fabricated on the base of high resistivity (1–2 kΩ cm) n-type oxidized silicon wafers with phosphorous-doped backside. Because the photolithographic patterning of the FTO film is difficult due to a high resistance of FTO film to acids, lift-off method was chosen for patterning. On the silicon dioxide layer previously by spray pyrolysis was deposited ITO or ZnO film that sufficiently easy can be etched in HCl solution. The active area of photodetectors after lift-off technological step was 50 mm^2. Current-voltage characteristic of photodetectors with 50 mm^2 area is shown in **Figure 12**.

5.1.1. Γ-Radiation detectors

The Γ-radiation detectors were designed on the base of the FTO-Si photodetectors with single crystal $Bi_4Ge_3O_{12}$ scintillator optically matched on the FTO electrode by silicon-based metal-organic lubricant. The optical matching of the photodetector with the scintillator is illustrated in **Figure 13**.

http://dx.doi.org/10.5772/67469

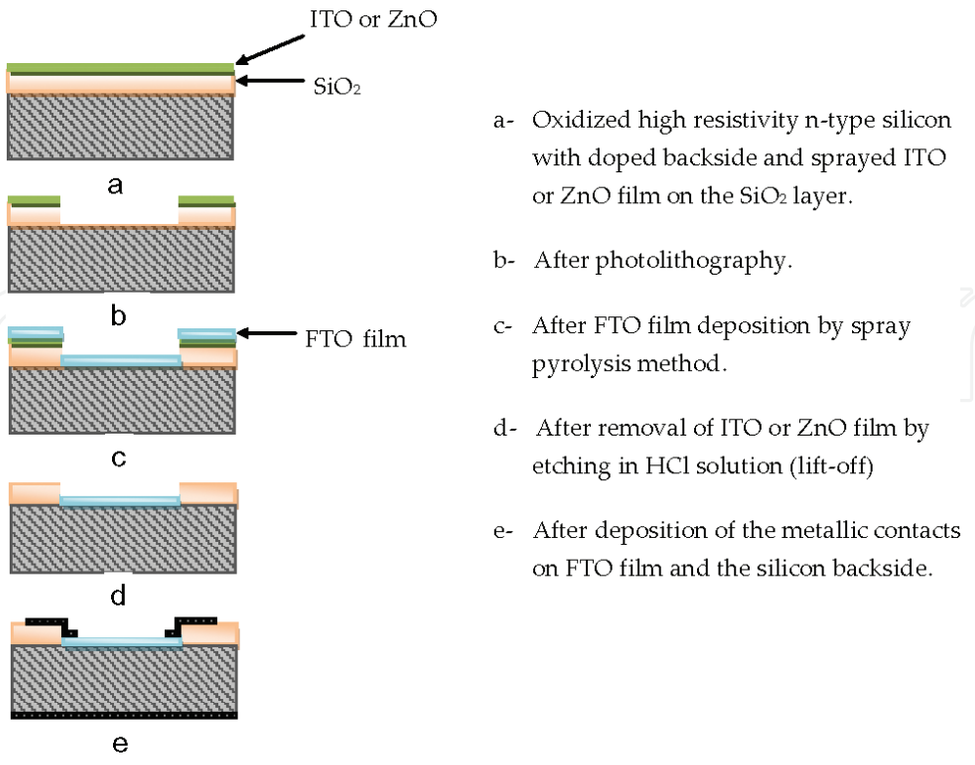

Figure 11. Technological fabrication steps of the FTO-Si photodetectors. (a) Oxidized high-resistivity n-type 350 μm thick silicon with doped backside and sprayed ITO or ZnO film on SiO_2 layer. (b) After photolithography. (c) After FTO film deposition by spray pyrolysis method. (d) After removal of ITO or ZnO film by etching in HCl solution (lift-off). (e) After deposition of the metallic contacts on FTO film and the silicon backside.

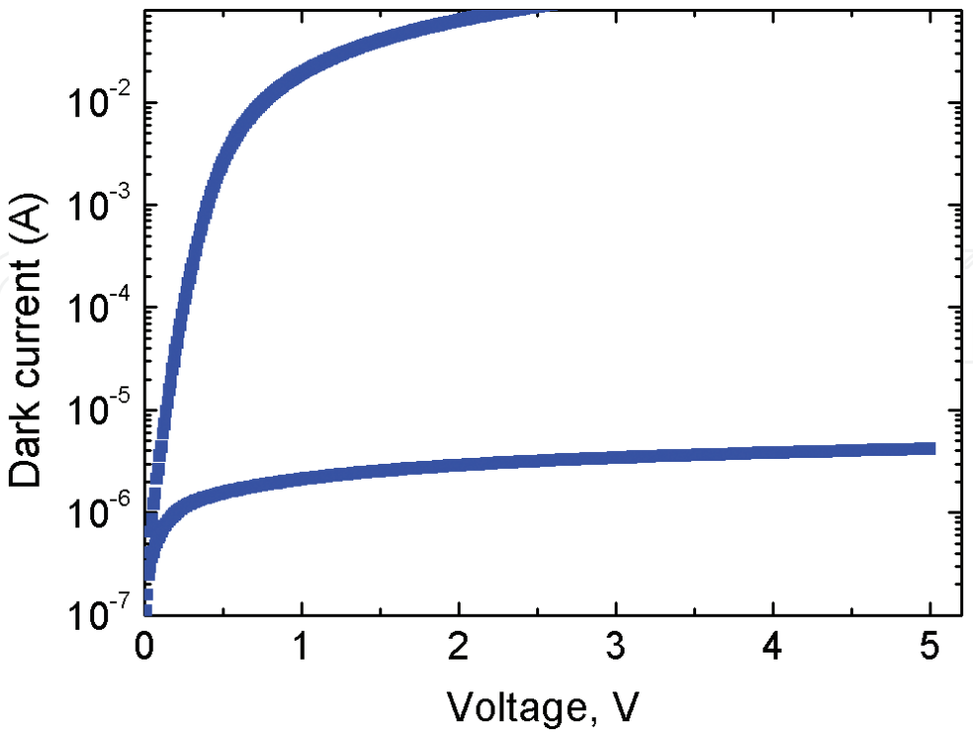

Figure 12. Current-voltage characteristic of FTO-Si photodetectors with 50 mm^2 area.

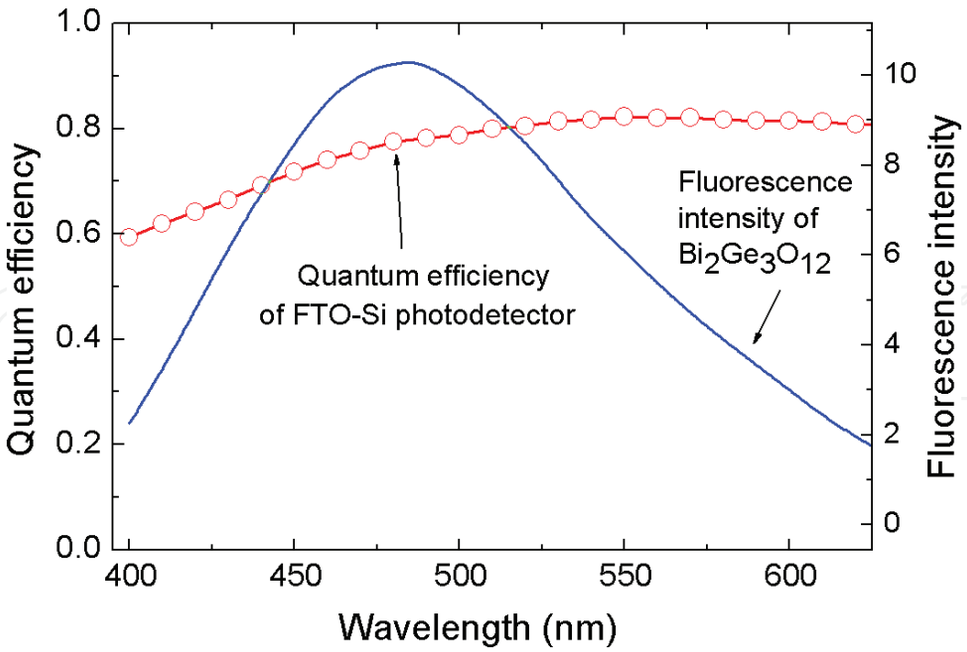

Figure 13. Illustration of optical matching of the photodetector with the scintillator.

Cooling of photodetectors up to 176 K reduces the dark current to a value around 10^{-10} A, while fluorescence lifetime of the scintillator (~ 3 ms) increases 10 times. Registration of low-level photocurrent produced by the photodetector under irradiation by γ-particles from ^{137}Cs was made by using a cooled preamplifier with noise of 250 e^- RMS.

Figure 14 shows recorded pulse height spectra when the photodetector with $Bi_4Ge_3O_{12}$ scintillator is irradiated from a137 Cs (Cs-137) source of γ-rays having energy of 661.5 keV. The registered signal is related to the main photon peak radiation from metastable nuclear isomer ^{137m}Ba (Ba-137). The energy resolution (FWHM/peak) is 16.5%. The FTO-Si photodetector with low noise amplifier was cooled to 176 K and operated at 5 V reverse voltage bias.

Figure 15 shows recorded pulse height spectra when the photodetector with $Bi_4Ge_3O_{12}$ scintillator is irradiated from 22Na (Na-22) source of γ-rays. The registered signals are related to two emission peaks, due to electron-positron annihilation (E_γ = 511 keV) and due to nuclear energy transition (E_γ = 1.27). The FTO-Si photodetector with low noise amplifier was cooled to 250 K and operated at 40 V reverse voltage bias.

Our silicon SB detectors of γ-rays fabricated by a simple and low-cost spray pyrolysis technique operate at low-voltage bias, and this is an advantage in comparison with much more expensive solid-state detectors based on cadmium telluride or mercuric iodide operating at reverse biases of order 100 V. Not cooled silicon detectors of γ-rays based on commercial Hamamatsu photodiodes (S1790-01) show low energy resolution of about 4% with 122 keV γ-rays from ^{97}Co radiation spectra [32].

http://dx.doi.org/10.5772/67469

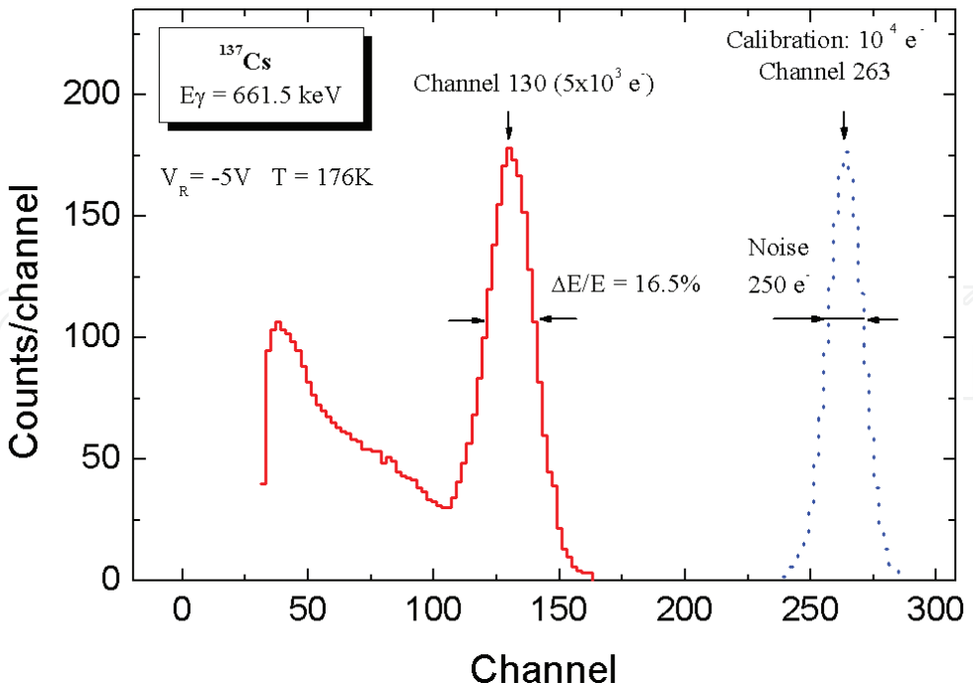

Figure 14. The pulse height spectra when $Bi_4Ge_3O_{12}$ scintillator is irradiated from 137Cs source of γ-rays having energy of 661.5 keV.

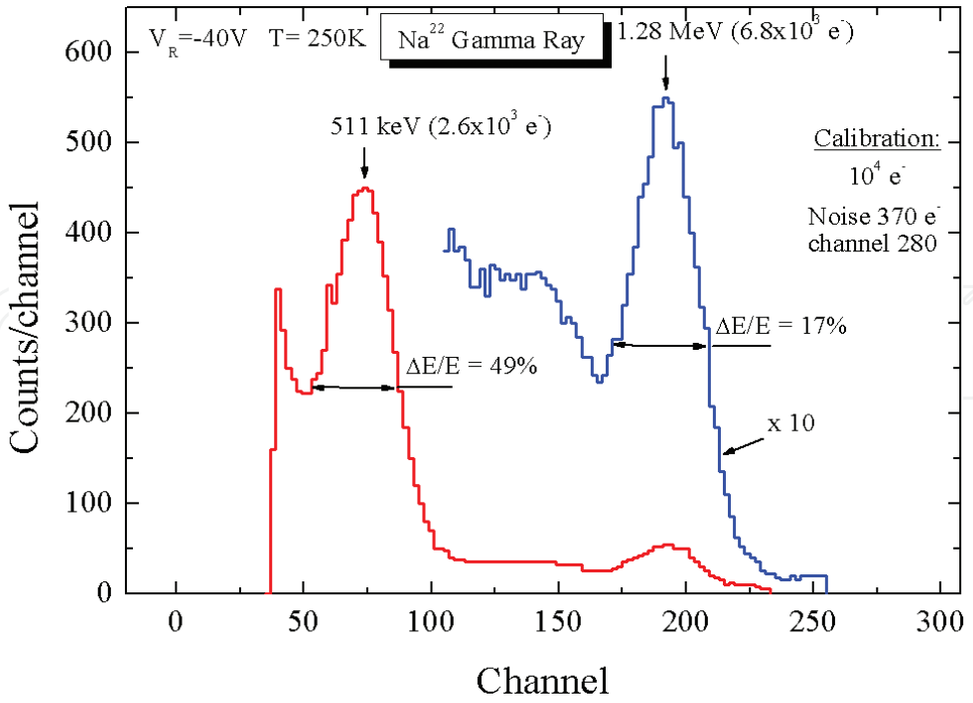

Figure 15. The pulse height spectra when $Bi_4Ge_3O_{12}$ scintillator are irradiated from 22Na source of γ-rays.

5.1.2. Radiation-resistant surface-barrier silicon photodetectors

Many technical applications require radiation-tolerant photodetectors that operate under high-energy particle irradiation, in particular under irradiation by reactor neutron at high flux of fast neutrons [33]. Commercial photodiodes such as the Hamamatsu Photonics photodiode S1723 was tested with respect to fast neutron radiation [34]. Significant changes of the leakage current and of the noise at a fluency of neutrons as low as 2.5×10^{10} n cm^{-2} were found. Damage also reduces the spectral sensitivity of the silicon photodiodes at long wavelengths due to a dramatic reduction of the minority lifetime.

Fast and radiation-resistant surface-barrier ITO-Si photodetectors have been fabricated using silicon epitaxial n-n^+ structures with 8 or 25 μm thick undoped epitaxial layer. The epitaxial layers with donor concentration 10^{13} cm^{-3} were grown by chemical vapor deposition on high-doped (10^{19} cm^{-3}) 300 μm n^+-silicon substrate. The silicon dioxide layer was grown on the surface of the epitaxial layer. An active device area (3–5 mm^2) was defined by chemically etching SiO_2 film. The ITO film as transparent conducting electrode with thickness of about 85 nm was deposited by spray pyrolysis method. A Cr/Ni metallic contact was deposited on the backside of n^+ substrate. The front metallic contact to ITO layer was created by the lift-off photolithography technique. After probing, the wafer with numerous fabricated devices was diced, and the chips were mounted on T0-8 body using silver epoxy.

The idea of the radiation-resistant photodiodes is based on existence of built-in electric field inside of the epitaxial silicon layer due to its nonuniform auto-doping as a result of the solid-state diffusion of antimony from the heavy-doped substrate during the growing process [35]. If built-in electric field is overlapped with the electric field inside the depletion layer, photogenerated minority carrier will be separated by a drift mechanism, and its recombination in defects formed by radiation will be negligible. Such photodetector will be high resistant to neutron flux even at zero bias.

An inhomogeneous impurity distribution of donors (N_D) inside the epitaxial layer estimated with capacitance-voltage (C-V) measurements [36] is shown in **Figure 16**, where the experimental points were approximated by two exponential curves (dotted lines). The doping variation in the epitaxial layer causes appearance of the built-in electric field $E = (kT/q)(1/N_D)(dN_D/dx)$.

The current-voltage characteristics of the ITO-Si photodetectors fabricated using 25 μm epitaxial silicon structures is shown in **Figure 17**.

In photodetectors with 25 μm epitaxial layer operating without voltage bias, a strong built-in electric field due to auto-doping effect does not overlapped with the electric field in depletion region. At that, part of photogenerated minority carriers needs to cross a distance without electric field by diffusion inside the epitaxial layer. However, after exposition under a neutron flux of about 10^{14} cm^{-3}, lifetime of the minority carriers is reduced from 36 μs to 12 ns, and photogenerated carriers recombine in this neutral area. For radiation resistance, thinner epitaxial layer needs to be used. **Figure 18** shows the spectral sensitivity of ITO-Si photodetectors at zero bias voltage fabricated on 8 μm epitaxial layers under irradiation by fast neutrons with flux of 3×10^{14} cm^{-2}.

http://dx.doi.org/10.5772/67469

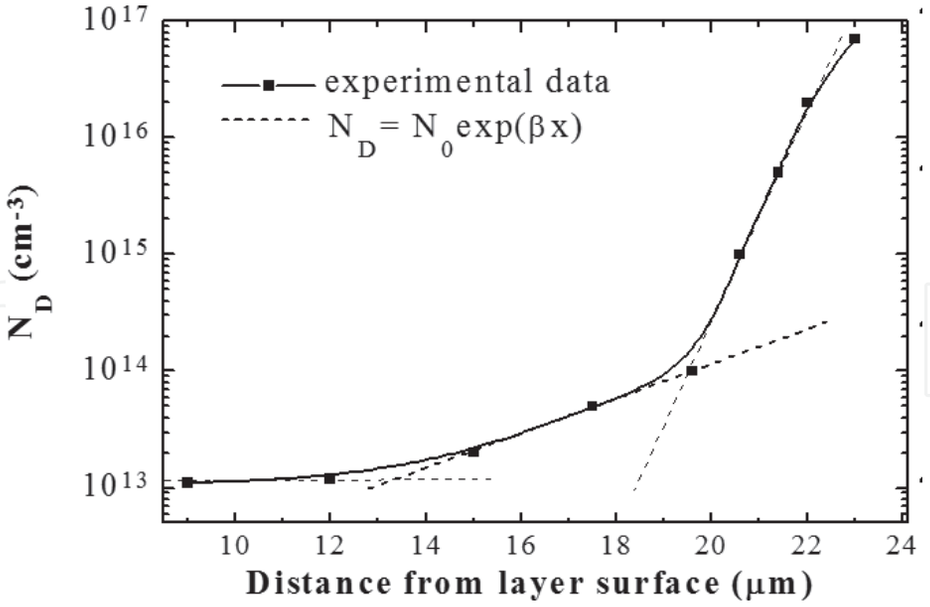

Figure 16. The donor concentration distribution inside the 25 μm epitaxial layer. Distance is shown from the epitaxial layer surface.

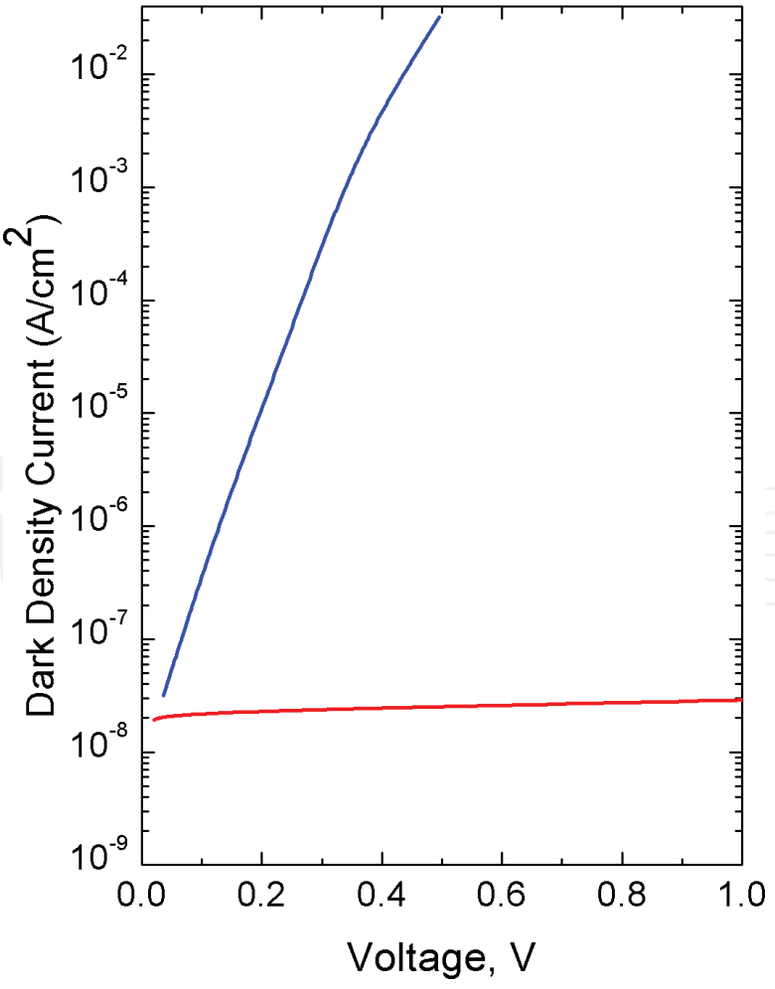

Figure 17. Current-voltage characteristics of ITO-Si photodetectors with an area of 3 mm^2.

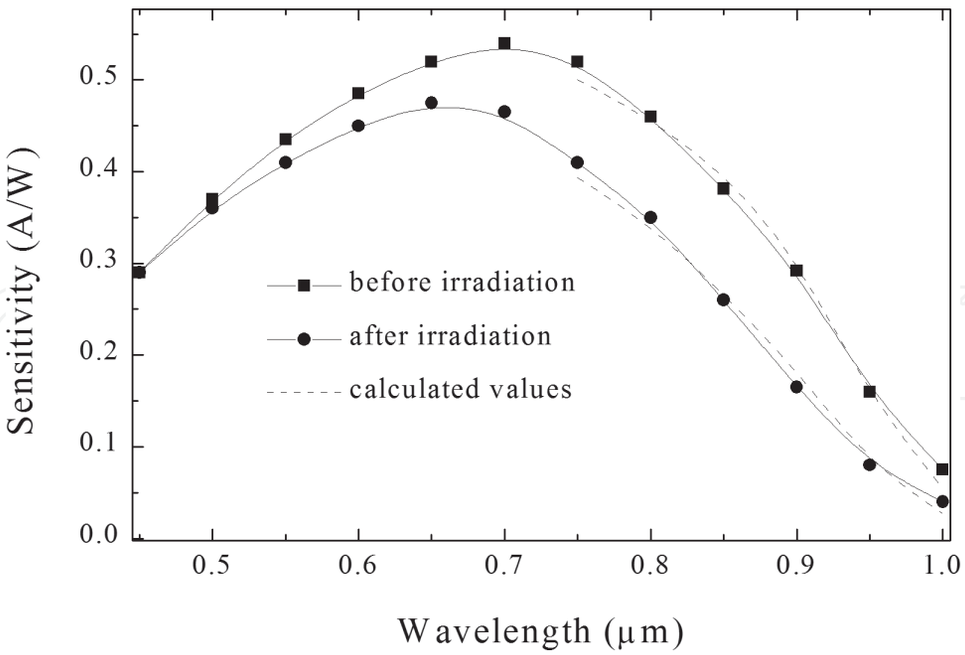

Figure 18. Spectral sensitivity of ITO-Si photodetectors at zero bias voltage fabricated on 8 μm epitaxial layers under irradiation by fast neutrons with a flux of 3×10^{14} cm^{-2}.

We suppose that ~20% reducing sensitivity of irradiated photodiodes in near-infrared spectral range is caused by lack of a contribution in photocurrent from carriers' photogenerated inside of heavy-doped silicon substrate. After neutron irradiation, such contribution is not significant in this spectral region due to a considerable shortage of the minority carrier lifetime. Thus, ITO-Si photodetectors with 8 μm epitaxial layers operating at zero voltage bias are extremely resistant to very big neutron flux. Photodetectors fabricated on the epitaxial layers with bigger thickness need to operate with the voltage bias. However, radiation damage produces an unacceptable level of the dark current because of dramatically reduction of the minority carrier lifetime. Devices with reported design can be used in optoelectronic equipment operating at hard radiation conditions without loss of their principal parameters.

6. Surface-barrier photodetectors for 1.3–1.55 μm

In this section, a new SB photodetector based on HgInTe-semiconductor compound. The development and improvement of fiber-optic communication system imply the use of high-speed and high-efficiency photodetectors. The transmission signal with a wavelength of 1.55 μm is especially important for long-distance communications. For this purpose, epitaxial layers of quaternary $In_xGa_{1-x}As_yP_{1-y}$ alloy with x = 0.57 and y = 0.95 are practically used for effective detector fabrication. Twenty-five years ago, the perspective of SB photodiodes based on $Hg_3In_2Te_6$ or mercury indium telluride (MIT) semiconductor has been shown [37–39]. The next years increasing interest in photodetectors based on this semiconductor [40–42]. The

http://dx.doi.org/10.5772/67469

$Hg_3In_2Te_6$ is a direct energy gap semiconductor with E_g = 0.72 eV at 300 K, close to germanium, and crystallizes in the zinc blend structure in which case 1/3 of all sites in the cationic sub-lattice are vacant. These stoichiometric vacancies with a concentration of about 10^{12} cm^{-3} determine unique properties of this semiconductor. It is inactive to dopants up to the doping concentration of 10^{20} cm^{-3} for fabrication p-n junctions, electrical properties of the MIT are indifferent to active defects [43], and material is high resistant to ionizing radiation [44]. The properties of the SB Au-MIT [40], Ni-MIT [41], and ITO-MIT [43] photodetectors were studied. In this section, electrical and optical properties of SB photodetectors on the base of the MIT single crystals with the ITO film as transparent conducting electrode deposited on chemically treated MIT surface are reported. Almost the same detectors in which the chemical treatment was changed on treatment in oxidizing RF plasma were patented recently in China [45], but their characteristics are not published.

The starting material for the photodetector fabrication was an *n*-type MIT mechanically and chemically polished wafer with carrier concentration of about 1×10^{13} cm^{-3}. The wafers were etched in 5% solution of Br_2 in N,N-dimethylformamide at the etching speed approximately of 0.3 μms^{-1}. The density of surface defects visible with a microscope was found as 30 cm^{-2}. After etching, wafers were boiled in azeotropic acetonitrile-based mixture and dried in N_2 atmosphere. The roughness of surface after the abovementioned polishing was determined as 0.03 μm.

The attempts to form a Schottky potential barrier on the MIT surface directly by the deposition of the ITO film lead to a weak rectifying nature of the ITO-MIT contact. The best rectifying characteristic has been observed if the ITO deposition was performed on a thin (0.02–0.03 μm) oxide layer chemically grown on the MIT surface. For chemical growth of oxide layer on the MIT surface, wafer was dipped on a few minutes in (1:1:1) solution prepared H_2O_2, N,N-dimethylformamide, and NH_4OH, previously heated to beginning of intensive foaming. The oxide thickness was measured using an ellipsometer. The chemically grown oxide composition was studied by X-ray photoelectron spectroscopy (XPS) [39]. Results of measurements are shown in **Figure 19**.

Analysis of XPS peaks corresponding the binding energies of the In $3d_{5/2}$, Te $3d_{5/2}$, and Hg 4f at 444.8 eV, 576.4 eV, and 100.7 eV, respectively, allows estimating the oxide composition: 40 at. % In_2O_3, 50 at. % TeO_2, and 10 at. % HgO. Almost the same oxide content was reported in Ref. [45], where the oxide layer was fabricated by RF plasma oxidation. The ITO film can be deposited on the oxide surface by spray pyrolysis technique or by sputtering.

In this work, we focused our attention on two SB photodetector types, fabricated on the thick (700 μm) and the thin (70 μm) MIT substrates. Typical current-voltage characteristic of ITO-oxide-MIT photodetectors with 3 mm^2 active area is shown in **Figure 20**.

Density of the dark current is almost the same as reported in [40, 41], but the spectral external quantum efficiency of the ITO-oxide-MIT photodetectors is more than 90% (**Figure 21**) and very differs from one reported for the Au-MIT [40] and Ni-MIT [41] Schottky-based photodetectors with 20–50% quantum efficiency.

Note that the quantum efficiency of ITO-MIT photodetectors with the ITO film deposited by sputtering on the MIT surface without specially created oxide layer is only about 60% [46].

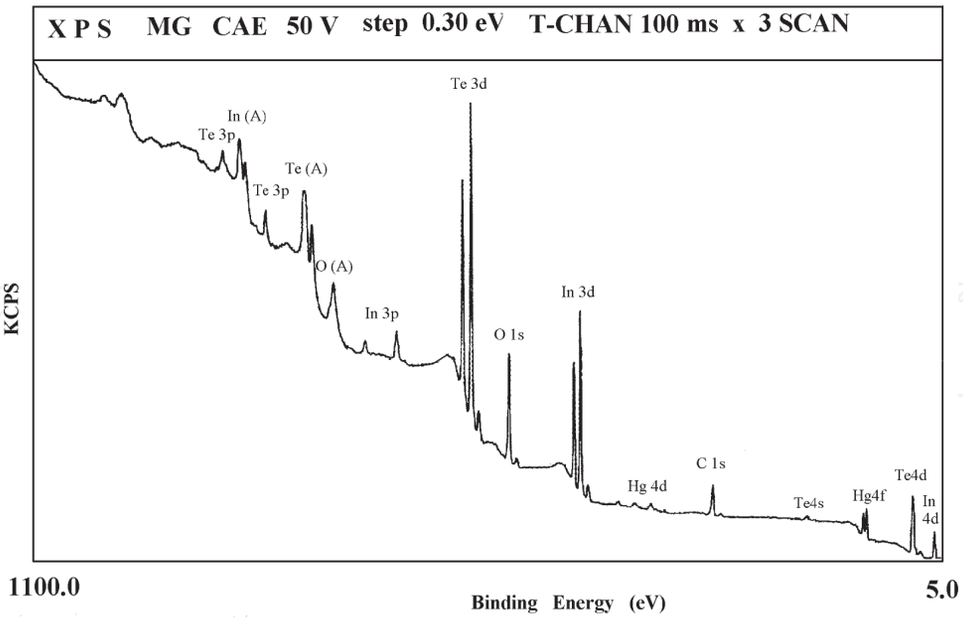

Figure 19. XPS spectrum of chemically grown oxide on the MIT surface.

The time response characteristic of the photodetectors fabricated using 70 μm thick MIT wafers measured at the reverse voltage bias of 120 V irradiated by laser pulse with 1.3 μm wavelength is shown in **Figure 22**.

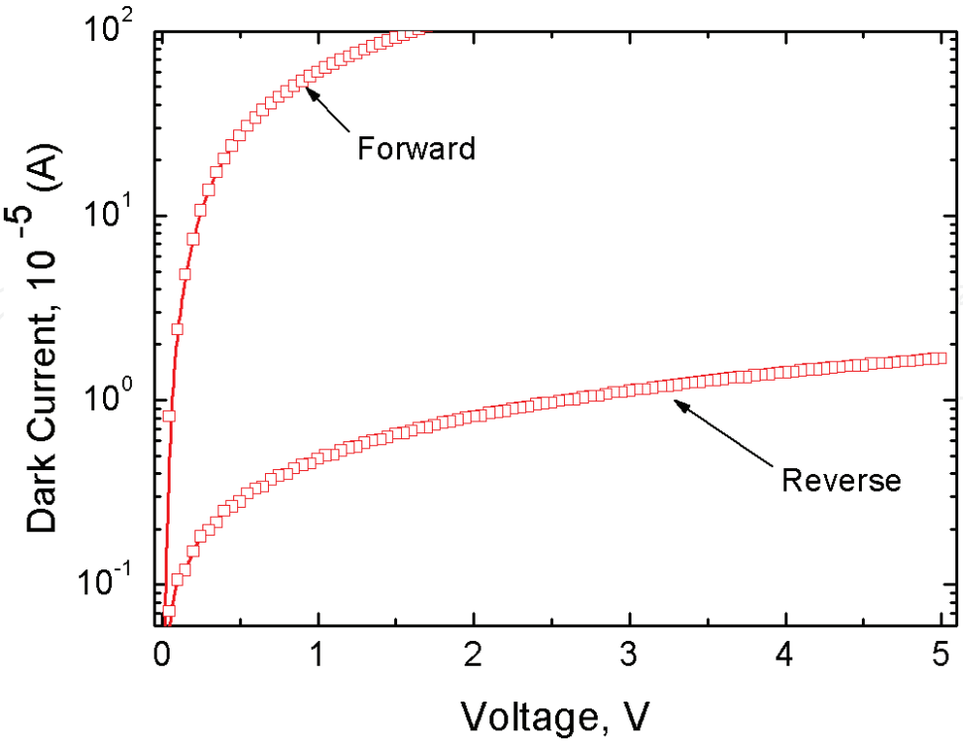

Figure 20. The current-voltage characteristic of ITO-oxide-MIT photodetectors with 3 mm^2 active area.

http://dx.doi.org/10.5772/67469

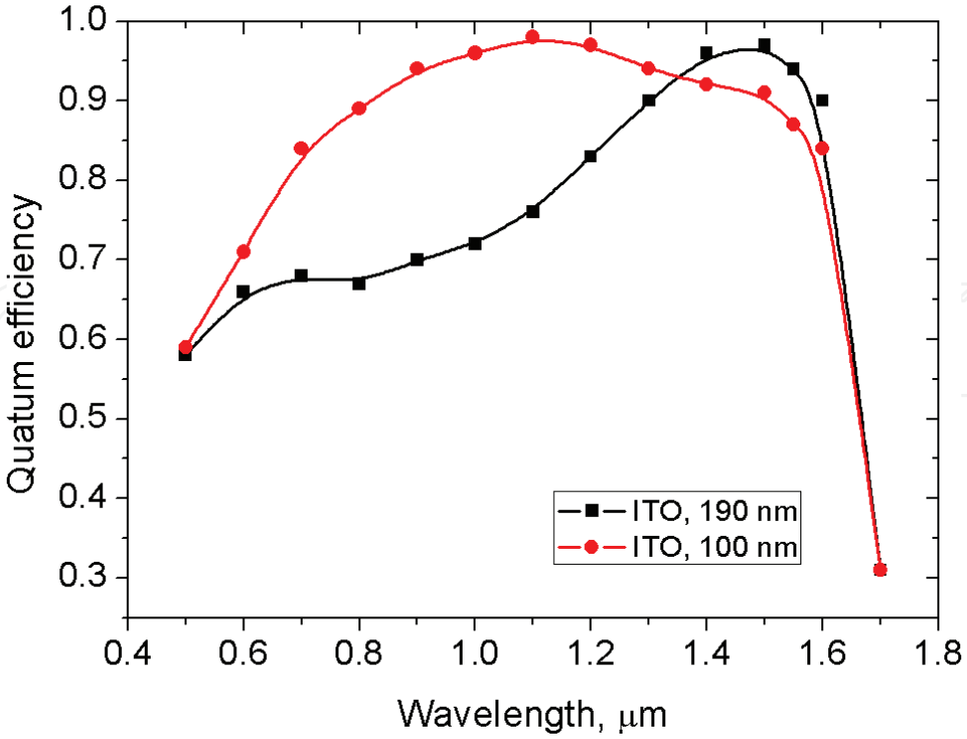

Figure 21. The spectral external quantum efficiency of the ITO-oxide-MIT photodetectors for two thicknesses of the ITO film.

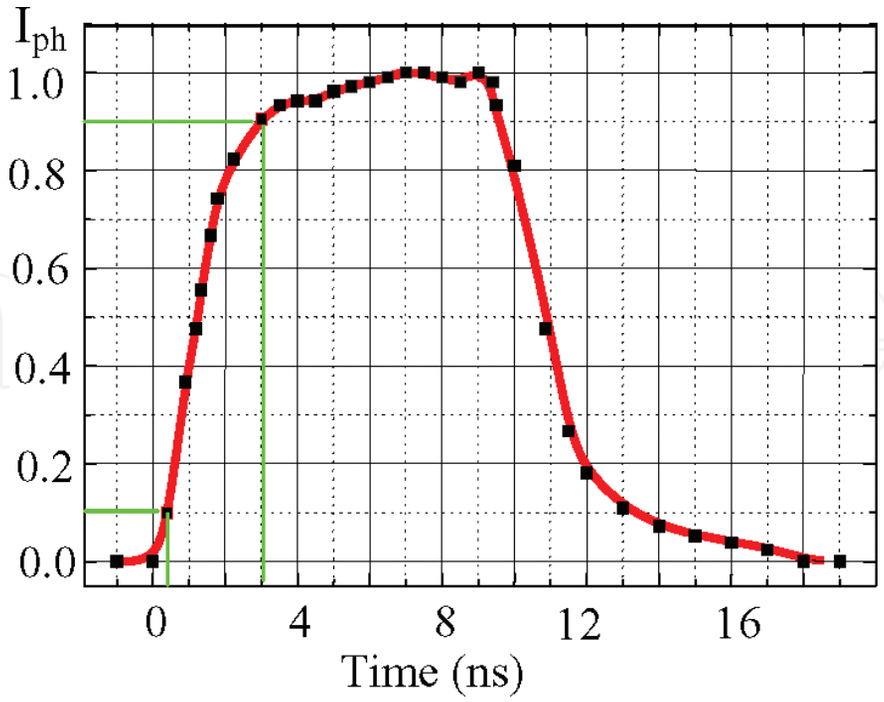

Figure 22. The time response characteristic of the 70 μm thick MIT photodetectors with 3 mm^2 area at a reverse voltage bias of 120 V irradiated by a laser pulse with 1.3 μm wavelength.

7. Conclusions

We presented the properties of surface-barrier photodiodes suitable for a wide spectral range and fabricated using a simple and low-cost spray deposition method that does not require expensive technological equipment. Of course, in this short report, it was not possible to describe in detail some technological aspects, such as the chemical treatment of the semiconductors used for the photodetectors. Readers can found further information in the works referenced in this chapter. The aim of this work was to review illustratively a simple technological method for the fabrication of high-efficiency surface-barrier photodiodes for applications in a wide spectral range, from UV to near infrared, using different semiconductor materials. This method has been successfully used for the fabrication of high-efficiency silicon solar cells whose characteristics have already been reported [47].

Author details

Oleksandr Malik* and Francisco Javier De la Hidalga-Wade

*Address all correspondence to: amalik@inaoep.mx

Electronics Department, Instituto Nacional de Astrofísica, Óptica y Electrónica (INAOE), Puebla, Mexico

References

[1] R. T. Tung. The physics and chemistry of the Schottky barrier height. Appl. Phys. Rev. 2014; 1: 1-55.

[2] S. J. Fonash. Solar cell device physics. Academic Press. NY 1981: 331 p. ISBN 0-12-261980-3.

[3] A. L. Dawar, J. C. Joshi. Review semiconducting transparent thin films: their properties and applications. J. Mater. Sci. 1984; 19: 1-23.

[4] J. DuBow, D. Burk, and J. Sites. Efficient photovoltaic heterojunctions of indium tin oxides on silicon. Appl. Phys. Lett. 1976; 29(8): 494-496.

[5] J. Manifacier, L. Szepessy. Efficient sprayed In_2O_3 n-type silicon heterojunction solar cell. Appl. Phys. Lett. 1977; 31; 459-462.

[6] T. Feng, A. K. Ghosh, and C. Fishman. Spray deposited high efficiency SnO_2-silicon solar cells. Appl. Phys. Lett. 1979; 35(3): 266-268.

[7] A. Malik, V. Baranyuk, and V. Manasson. Solar cells based on the SnO_2-SiO_2-Si heterojunction. Appl. Sol. Energy. 1979; 2: 83-84. ISSN: 0003-701x.

[8] A. Malik, V. Baranyuk, and V. Manasson. Improved model of solar cells based on In_2O_3/SnO_2-SiO_x-nSi structures. Appl. Solar Energy. 1980; 1:1-2.

[9] S. Ashok, P. Sharma, and S. Fonash. Spray-deposited ITO-silicon SIS heterojunction solar cells. IEEE Trans. Electron. Dev. 1980; ED-27(4): 725-730.

[10] O. Malik, F. J. De la Hidalga-W, C. Zúñiga-I, and G. Ruíz-T. Efficient ITO-Si solar cells and power modules fabricated with a low temperature technology: results and perspectives. J. Non Cryst. Solids. 2008; 354: 2472-2477.

[11] O. Malik, F. J. De la Hidalga-W, C. Zúñiga-I, and G. Ruíz-T. Efficient ITO-Si solar cells and power modules fabricated with a low temperature technology: results and perspectives. J. Non Cryst. Solids. Elsevier. 2008; 354: 2472-2477.

[12] J. B. Mooney, S. B. Radding. Spray pyrolysis processing. Ann. Rev. Mater. Sci. 1982; 12: 81-101.

[13] O. Malik, F. J. De la Hidalga-Wade. Comparison of tin-doped indium oxide films fabricated by spray pyrolysis and magnetron sputtering. Cryst. Res. Technol. 2015; 50(7): 516-521.

[14] O. Malik, F. J. De la Hidalga-Wade, and R. Ramírez Amador. Fluorine-doped tin oxide films with a high figure of merit fabricated by spray pyrolysis. J. Mater. Res. 2015; 30(13): 2040-2045.

[15] G. Haacke. New figure of merit for transparent conductors. J. Appl. Phys. 1976; 47: 4086-4089.

[16] E. Burstein. Anomalous optical absorption limit in InSb. Phys. Rev. 1954; 93: 632-633.

[17] A. Malik, A. Seco, E. Fortunata, and R. Martins. New UV-enhanced solar blind optical sensors based on monocrystalline zinc sulphide. Sens. Actuators A. 1998; 67: 68-71.

[18] V. Machnii, A. I. Malik, and N. Melnik. Solar blind photodiode based on ITO/ZnS heterostructures. Sov. Phys. Tech. Phys. 1990; 60: 146-147.

[19] D. Caputo, G. de Cesare, F. Irrera, and F. Palma. Solar-blind UV photodetectors for large area applications. IEEE Trans. Electron. Devices. 1966; 43: 1351-1356.

[20] A. I. Malik, G. G. Grushka. Optoelectronic properties of metal oxide-gallium phosphide heterojunctions. Sov. Phys. Semicond.. 1991; 25(10): 1017-1020. ISSN 0038-5700.

[21] A. Malik, A. Seco, E. Fortunato, R. Martins, B. Shabashkevich, and S. Piroszenko. A new high ultraviolet sensitivity FTO-GaP Schottky photodiode fabricated by spray pyrolysis. Semicond. Sci. Technol. 1998; 13: 102-107.

[22] Yu. Vygranenko, A. Malik, M. Fernandes, R. Schwarz, and M. Vieira. UV-Visible ITO/GaP photodiodes: characterization and modeling. Phys. Status. Sol. A. 2001; 185(1): 137-144.

[23] A. I. Malik, B. Shabashkevich, and S. Piroszenko. Photodiode for the ultraviolet spectral range. Patent of Ukraine N. 71544.

[24] O. Malik, F. J. De la Hidalga-Wade, C. Zuniga-Islas, and J. Abundus Patiño. UV-sensitive optical sensors based on ITO-gallium phosphide heterojunctions. Phys. Status Sol. C. 2010; 7(3-4): 1176-1179.

[25] A. N. Pikhtin, S. A. Tarasov, and B. Kloth. Ag-GaP Schottky photodiodes for UV sensors. IEEE Trans. Electron. Dev. 2003; 50(1); 215-217.

[26] V. C. Boutenko, Y. G. Dobrovolskiy, S. I. Piroszenko, B. Shabashkevich, V. G. Yoriev. Radiometer of power luminosity in the ultraviolet spectral range. Patent of Ukraine N. 82843.

[27] E. Ahlstrom. W. W. Gartner. Silicon surface barrier photocells. J. Appl. Phys. 1962; 33(8): 2602-2606.

[28] A. J. Tuzzolino, E. L. Hubbard, M. A. Perkins, and C. Y. Fan. Photoeffects in silicon surface-barrier diodes. J. Appl. Phys. 1962; 33(1): 148-155.

[29] H. Kato, J. Fujimoto, T. Kanda, A. Yoshida, and T. Arizumi. SnO_2-Si photosensitive diodes. Phys. Status Sol. A. 1975; 32: 255-261.

[30] A. Malik, R. Martins. Metal oxide/silicon heterostructures: new solution for different optoelectronic applications. MRS Proc. 1997; 487: 375-380.

[31] A. Malik, M. Vieira, and M. Fernandes. Surface-barrier Si-based photodetectors fabricated by spray pyrolysis technique. Philosophical Mag. B. 2000; 80(4); 781-790.

[32] C. Bilton, S. Hedges, P. R. Hobson, and D. C. Imrle. Low-cost silicon photodiodes for X-ray detection. J. Phys. E Sci. Instrum. 1988; 21: 809-811.

[33] M. Hasegawa, S. Mori, T. Ohsugi, H. Kojima, A. Taketani, T. Kondo, and M. Noguchi. Radiation damage of silicon junction detectors by neutron irradiation. Nucl. Instrum. Methods. 1989; A277: 395-400.

[34] W. Dabrowski, K. Korbel, and A. Skoczeń. Fast neutron damage of silicon PIN photodiodes. Nucl. Instrum. Methods Phys. Res. A. 1991; 301(2): 288-294.

[35] B. A. Joyce, J. C. Weaver, and D. J. Maule. Impurity redistribution processes in epitaxial silicon layers. J. Electrochem. Soc. 1965; 112(11): 1100-1106.

[36] P. J Baxandall, D. J Colliver, and A. F Fray. An instrument for the rapid determination of semiconductor impurity profiles. J. Phys. E Sci. Instrum. 1971; 4: 213-221.

[37] A. I. Malik, G. G. Grushka, and N. R. Tevs. High-efficiency measuring photodiodes based on mercury indium telluride. Sov. Tech. Phys. 1990; 35: 723-726.

[38] A. I. Malik, G. G. Grushka. Self-calibrated radiometric IR photodiode based on the defect semiconductor $Hg_3In_2Te_6$ for the spectral range 0.85-1.5 μm. Sov. Tech. Phys. 1990; 35: 1227-1231.

[39] A. I. Malik, M. Vieira, M. Fernandes, F. Macarico, and Z. Grushka. Near-infrared photodetectors based on HgInTe-semiconductor compound. Proc. SPIE. Photodetectors: Materials and Devices IV. 1999; 3629: 433-442.

[40] L. A. Kosyachenko, Yu. S. Paranchich, V. N. Makagonenko, V. M. Sklyarchuk. E. F. Sklyarchuk, and I. I. German. Electrical performance of HgInTe surface-barrier photodiodes. Tech. Phys.. 2003; 48(5): 647-650.

[41] L. A. Kosyachenko, I. S. Kabanova, V. M. Sklyarchuk, O. F. Sklyarchuk, and I. M. Rarenko. $Hg_3In_2Te_6$-based photodiodes for fiber optic communication. Phys. Status Solidi A. 2009; 206(2): 351-355.

[42] L. Zhang, X. L. Zhang, W. G. Sun, and Z. X. Lu. Proc. SPIE. 2011; 8193: 1-6.

[43] O. L. Maslyanchuk, L. A. Kosyachenko, I. I. German, I. M. Rarenko, V. A. Gnatyuk, and T. Aoki. Electrical and optical properties of $Hg_3In_2Te_6$ single crystals. Phys. Status Solidi C. 2009; 6(5): 1154-1157.

[44] O. G. Grushka, V. T. Maslyuk, S. M. Chupyra, O. M. Mysliuk, S. V. Bilichuk, and I. I. Zabolotskiy. The effect of irradiation with electrons on the electrical parameters of $Hg_3In_2Te_6$. Semiconductors. 2012; 46(3): 312-314. ISSN 10637826.

[45] Te-In-Hg photoelectronic detector chip manufactured method. Patent of China N. CN101060144A 2014.

[46] L. A. Kosyachenko, I. M. Rarenko, E. F. Sklyarchuk, I. I. German, and Sun Weiguo. Electrical characteristics of the ITO/HgInTe photodiodes. Semiconductors. 2006; 40(5): 554-557.

[47] O. Malik, F. J. De la Hidalga-W. Physical and technological aspects of solar cells based on metal oxide-silicon contacts with induced surface inversion layer. In: Application of solar energy, R. Rugescu Editor. 2013. Intech, Croatia. ISBN 978-953-51-0969-3.

IntechOpen